Smart Structures and Systems, Vol. 3, No. 3 (2007) 357-372
DOI: http://dx.doi.org/10.12989/sss.2007.3.3.357

Parametric density concept for long-range pipeline health monitoring

Won-Bae Na†

Department of Ocean Engineering, Pukyong National University, Busan, Korea

Han-Sam Yoon‡

Research Center for Ocean Industrial Development, Pukyong National University, Busan, Korea

(Received October 30, 2006, Accepted January 9, 2007)

Abstract. Parametric density concept is proposed for a long-range pipeline health monitoring. This concept is designed to obtain the attenuation of ultrasonic guided waves propagating in underwater pipelines without complicated calculation of attenuation dispersion curves. For the study, three different pipe materials such as aluminum, cast iron, and steel are considered, ten different transporting fluids are assumed, and four different geometric pipe dimensions are adopted. It is shown that the attenuation values based on the parametric density concept reasonably match with the attenuation values obtained from dispersion curves; hence, its efficiency is proved. With this concept, field engineers or inspectors associated with long-range pipeline health monitoring would take the advantage of easier capturing wave attenuation value, which is a critical variable to decide sensor location or sensors interval.

Keywords: pipelines monitoring; guided waves; attenuation; parametric density.

1. Introduction

Pipelines, used for transporting petrochemicals, water and other necessities, are major infrastructures for human being's daily life. Failure free performance of these pipes is desired since any malfunction can cause something as minor as an inconvenience to something tragic as loss of human life and severe environmental damage. The extreme event of pipeline malfunction would be pipeline leak, which is initially caused by corrosion, metal loss, mechanical damage, etc. With increasing awareness and concern for the environment, recent pipeline leak incidents, mainly caused by irregular inspection and monitoring, have shown that the cost is much more than the associated downtime and clean-up expenses. An effective leak detection program will easily pay for itself through reduced spill volume and increased public confidence. Leak detection technology has been developed to a sophisticated level of automation for onshore gas and liquid transmission pipelines, and this technology is routinely applied for shallow water offshore or buried pipelines. However, deepwater, underground, and arctic flowlines operate under condition rarely encountered in the previous development schemes. These

†Assistant Professor, Corresponding Author, E-mail: wna@pknu.ac.kr
‡Lecturer

applications are typified by extremely high flow rates of full well stream, multiphase fluids and flow over lengths that are well beyond our experience (Scott and Barrufet 2003). Therefore, a new concept of pipeline leak detection has been required. One of those ways is applying structural health monitoring concept, which needs higher technology to pursue its completeness. Structural health monitoring (SHM) aims to give a diagnosis of the state of the constituent materials, of the different parts, and of structure itself (Balageas 2006). In addition to diagnosis, SHM involves the integration of sensors, data transmission, computational power, and processing ability inside structures.

In present, long-range pipeline health monitoring for detecting pipeline leak and defects is more demanded because of the increasing cost of water, petrochemical fluids, and environmental recovery. Basic idea of the long-range pipeline health monitoring is installing long-live sensors on the pipelines, using their output signals to check the healthy state of the pipelines. Here, the success of the long-range pipeline health monitoring depends on the sensors used, the communication tools adopted, and the signal analysis implemented. The durability and functionality of the sensors are mainly concerned, at least one way communication should be readable, and an exact and economic signal analysis is highly needed. In addition, for the long-range pipeline health monitoring, the location of the monitoring sensors is significant. The interval between those sensors should be well designed otherwise the operation of semi-permanently installed sensors would be difficult.

There are different types of sensors are available for the long-range pipeline health monitoring such as cable sensors, fiber optic sensors, ultrasonic sensors, vapor-monitoring sensors, and guided-wave sensors. Among them, the guided wave sensors are ones of most available sensors for long-range pipeline health monitoring, mainly due to their long-range inspection capability. In addition, it is not necessary to remove insulation except in a small area where the guided-wave sensors are placed. Several vendors offer versions of guided wave technology that use either piezoelectric or electromagnetic guided wave sensors or probes. Regardless of which guided wave sensor type is used, the physics of wave propagation, wave interaction with defects, and wave attenuation is the same (Kwun and Crouch 2006).

The guided wave technology can be also classified on how the sensors are located, and how launching and receiving signals. In the first class, the guided wave based monitoring involves installing a ring array of piezoelectric transducers or a thin strip of magnetostrictive material as the guided wave probe around the pipe circumference, launching a pulse of guided waves along the pipe, and receiving signals back from defects and welds. In the case, only one guided wave probe is used and the probe location is moving as the monitoring is forwarding. In the second class, the guided wave monitoring uses two guided wave probes along the line being tested, the first probe is launching a pulse of guided waves along the pipe, and then the second probe receiving signals from defects and welds. In either case, the sensors can be installed on the pipelines as a semi-permanent manner to operate long-term health monitoring activities. Because of the ability of the guided wave technology to monitor a long length of piping rapidly, this technology is now widely used for inspection or monitoring of pipeline networks and long-range pipelines, in particular for detection of corrosion, leaks, metal-loss etc.

Because of its long-range inspection capability on aboveground piping, the guided wave method was also thought to be a good solution for inspecting buried or underwater pipelines. Therefore, from the early stages of the guided wave technology development, efforts were also made to extend the applicability of the technology to buried or underwater pipelines, and to determine the inspection capabilities achievable on such pipelines. The main difference between most aboveground and underground or underwater pipelines is the presence of coating and surrounding soil or water. In typical buried or underwater pipelines, the guided wave propagating along the line undergoes a significant attenuation, the degree of which is dependent on various factors, including wave frequency, pipe coating, depth of burial, nature

of the surrounding medium, and the type of transporting fluid inside. Since the guided wave amplitude decays exponentially with the attenuation coefficient and distance, one cannot simply increase the drive power or the receiver sensitivity to overcome high attenuation and make substantive increases in range for a given size defect. Moreover, since the noise floor of the system ultimately limits the received information, one cannot use signal analysis to increase the range when the signals are decayed down to the noise level (Kwun and Crouch 2006). Therefore, a careful guided wave mode selection for a specific inspection purpose should be carried out (Wilcox, *et al*. 2001, Pan, *et al*. 1999). The mode selection depends on not only on inspection quality but also on long-range inspection capability. In other words, the selection of a particular mode should count on its sensitivity to the defects, which are sought and its ability to travel over a long distance without significant energy loss (Rose, *et al*. 1994). Thus, obtaining the attenuation of guided wave is a significant procedure to select a proper wave mode and finally to locate the monitoring sensors and their intervals in a proper manner.

With those backgrounds above, this study concerns about how one can obtain the attenuation of ultrasonic guided waves. Here, 'ultrasonic' guided wave is considered since this work focuses on guided wave propagating underwater pipelines; it should be also noted here that water is a perfect coupling medium for ultrasonic wave propagation. The word 'guided' is used since the ultrasonic waves are guided by cylindrical waveguide, which is a hollow cylinder (pipe). Similar works for pipelines have been done by several investigators (Alleyne and Cawley 1996, Kwun, *et al*. 1999, Guo and Kundu 2001, Aristégui, *et al*. 2001, Na and Kundu 2002, Kwun, *et al*. 2004, Na, *et al*. 2005). Those works mainly focus on attenuation dispersion curves, wave mode selections, etc. They obtained attenuation values from cumbersome numerical calculations and some of them used these values to decide sensors interval. Here, parametric density concept is proposed for a simpler attenuation calculation. This concept is initially proposed by Na, *et al*. (2006), but their application is limited for a steel pipeline. Therefore, this study is a kind of extension and more restrict verification of the parametric density concept for broader applications. For the study, three different pipe materials such as aluminum, cast iron, and steel are considered, ten different transporting fluids are assumed, and four different geometric pipe dimensions are adopted. It is shown that the attenuation values based on the parametric density concept reasonably match with the attenuation values obtained from dispersion curves; hence, its efficiency is proved. With this concept, field engineers or inspectors associated with long-range pipeline health monitoring would take the advantage of easier capturing wave attenuation value, which is a critical variable to decide sensor location or sensors interval.

2. Guided wave

The guided wave propagation in rods and hollow cylinders is analogous to that in plates. The horizontally polarized shear and symmetric modes of plate have their analogous in torsional and longitudinal wave modes. The anti-symmetric plate modes are analogous to the flexural modes of cylinders. It is possible to consider each type of motion separately and derive frequency equations for torsional, longitudinal, and flexural modes. However, it is also possible to develop a general frequency equation for the problem and then to resolve it into various modes. This was done by Gazis (1959a, 1959b) in the analysis of hollow cylinders. Meeker and Meitzler (1972), following the approach of Gazis, developed the Pochhammer-Chree equations for a solid cylinder in this manner. Detail information on this technique can be found in Achenbach (1984), Kolsky (1963), Onoe, *et al*. (1962), and Rose (1999).

More difficult problem is the problem of leaky guided waves in cylinders; it involves complex Bessel functions in the modeling. For solving this problem, many works have been performed by several investigators (Kumar 1971, Nagy 1995, Rose, *et al*. 1994). Most works on wave propagation in leaky cylindrical system involve two elastic solids - in one the wave propagates; it leaks in the second one. Recently, an expanded work for a general system was investigated by Pavlakovic and Lowe (2001). The full derivation of a model for wave propagation in multi-layered isotropic (elastic or viscoelastic) cylinder is well documented in references (Pavlakovic and Lowe 2001, Pavlakovic, *et al*. 1997). Here, the brief derivation of the model for wave propagation in multi-layered isotropic cylinder is introduced.

Given a three-layered cylinder, an inner material and an intermediate material represent finite layers and a surrounding material represents infinite space surrounding the cylinder. The partial waves at each layer combine to from a guided wave and the cylindrical system is assumed axisymmetric and infinitely long. From the Navier's displacement equation after some algebraic manipulations, the displacement field in terms of potential functions can be expressed. Then, using stress-strain and strain-displacement relations, the stresses in the boundary conditions can be obtained. After substituting the solutions of the potential functions into the displacement and stress fields, six equations in terms of six unknown partial wave amplitudes can be obtained (Pavlakovic and Lowe 2001). Then, we can assemble a 6 by 6 matrix from the six equations for the displacement ($\bar{u}$) and pertinent stresses ($\bar{\sigma}$) in terms of the partial waves. Finally, we can get the following equation,

$$\begin{Bmatrix} \bar{u} \\ \bar{\bar{\sigma}} \end{Bmatrix} = [D]\{A\} \tag{1}$$

The resulting matrix $[D]$ is called a material layer matrix and $\{A\}$ is a vector of partial wave amplitudes. The material layer matrix expresses all of the displacements and stresses that are required to evaluate boundary conditions such as solid-solid, solid-fluid, and fluid-fluid. Eq. (1) is used to assemble an equation that represents the entire system by using the global matrix method, which was first proposed by Knopoff (1964) and subsequently developed by researchers (Randall 1967, Schmidt and Jensen 1985, Mal 1988, Lowe 1995),

$$[G]\{A\} = 0 \tag{2}$$

where, $[G]$ is the global matrix. For nontrivial solution of $\{A\}$, the following condition must be satisfied.

$$Det[G] = 0 \tag{3}$$

The frequency, wavenumber, and attenuation values determine whether Eq. (3), characteristic equation is met, and need to be found via an iterative procedure. Roots of this characteristic equation give dispersion curves.

3. Attenuation

Attenuation caused by material damping may be specified in several ways. In each case, the damping values correspond to the exponential decay of plane waves in an infinite medium, and they are defined independently for the bulk waves. In general, there are three ways for the specification, hysteretic

structural damping, hysteretic damping (per meter), and Kelvin-Voigt viscous damping. Hysteretic structural damping defines a damping loss, which is a constant per wavelength traveled. It may be expressed in units of either Nepers per wavelength or dB per wavelength. A neper is an exponential decay constant, such that in the following equation,

$$A_{(location2)} = A_{(location1)}e^{-\alpha n} \tag{4}$$

Here, the amplitude of the wave, A, decreases by the factor $e^{-\alpha n}$ if α is in nepers per wavelength, and location 2 is n wavelengths downstream from location 1. For this type of damping, it follows that the loss per unit distance traveled increases as the frequency increases and the wavelength diminishes. Hysteretic damping (per meter) for convenience enables the bulk attenuation to be defined as a loss per unit distance at a given frequency. This then can be converted to the appropriate loss per wavelength; hence, it is identical to hysteretic structural damping in most senses (Pavlakovic and Lowe 2001). Kelvin-Voigt viscous damping defines the dashpot damping model, which is the damping force is proportional to the particle velocity. This model results in a bulk wave attenuation, which is a stronger function of frequency than the hysteretic damping. The loss per wavelength is now no longer constant but increases linearly with frequency. Accordingly, if the loss is expressed per unit distance then it increases with the square of the frequency. In order to define the attenuation one must specify a loss per unit distance at a particular frequency. In this study, the hysteretic structural damping is assigned to the bulk wave attenuation; this attenuation value is used to calculate guided wave attenuation.

In a perfectly elastic system that is surrounded by vacuum, the attenuation of guided wave is always be zero and therefore does not need to be considered. However, whenever damping materials are present or the system is surrounded by a liquid or solid medium, there is a mechanism for energy to be lost from the guided waves; hence, the solution in general includes attenuation, which is a property of the guided wave, just as much as phase velocity. In this study, the pipes are aluminum, cast iron and steel, which are less damping material so that the attenuation is mainly caused by the surrounded materials and sink. In case of a fluid-filled pipe, there are two ways to model the system: through a system without sink and one with sink (Na, *et al*. 2005). In strict words, for a pipe filled with a perfect fluid, the model with sink does not correctly represent the system. Some ultrasonic test designed to propagate energy through the fluid inside a pipe have not to use the sink. However, there is valuable information in the dispersion curves obtained by the second method when we are sending waves through the walls of the pipe. This is done when inspecting for anomalies in the pipe or when it not easy gaining access to the inside of the pipe. For such cases, it is useful to plot the dispersion curves for the pipe without complicating the dispersion curves with additional fluid modes such as standing wave modes due to the fluid. In addition, the sink model would be a more realistic when the radiated waves are not properly reabsorbed by the opposite wall of the pipe. Fluid filled pipes containing absorbing or scattering materials or being partially filled would be the examples (Pavlakovic and Lowe 2001). For this study, we assume sink for excluding all standing wave modes because the monitoring sensors are to be installed outside the pipes and the cylindrical guided waves assumed to propagate through the pipe walls. For the numerical calculation, a sink is placed at the centerline of the system by representing the waves in the internal fluid not by standing Bessel functions but by incoming Hankel functions. The sink absorbs the energy that propagates inwardly from the pipe and prevents the fluid modes from building up. The attenuation values are generally larger for this case because energy is lost in both the sink and the external fluid.

4. Numerical calculation

Based on the numerical scheme derived from Pavlakovic and Lowe (2001), numerical calculation is done for the models shown in Figs. 1, 2, and 3. Three different pipe materials such as aluminum, cast iron, and steel are considered, and their material properties are shown in Table 1. The inner radii, 2 mm and 2.5 mm, of the pipes are initially assumed and the pipe wall thickness is fixed to 1 mm. Thus, the ratio of the radius to the wall thickness is 2 to 1 or 2.5 to 1. The surrounding material is assumed water and the inside filling fluids are shown in Table 2. We considered total ten different inside filling fluids to compare the attenuation values of the guided waves. For all cases, sink is assumed for the numerical calculation. It should be emphasized here that the first longitudinal wave mode, L(0,1), is only considered for the numerical calculation because this mode is known one of the most important guided wave modes for guided wave studies. Other fundamental modes such as flexural, F(1,1), and torsional, T(0,1), would be considered important but not studied here. That is, this study presented here is concerned solely with the attenuation of L(0,1) mode. For this reason, it is implicitly assumed through that a suitable transducer can be designed so that single mode excitation can be obtained at any operating point.

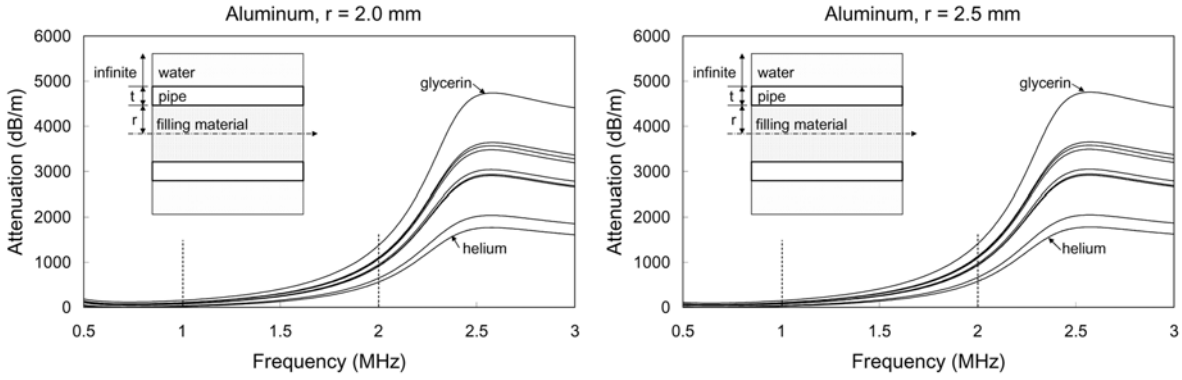

Fig. 1 Frequency vs. attenuation dispersion curves for aluminum pipe with 2.0 mm (left) and 2.5 mm (right) inner radius

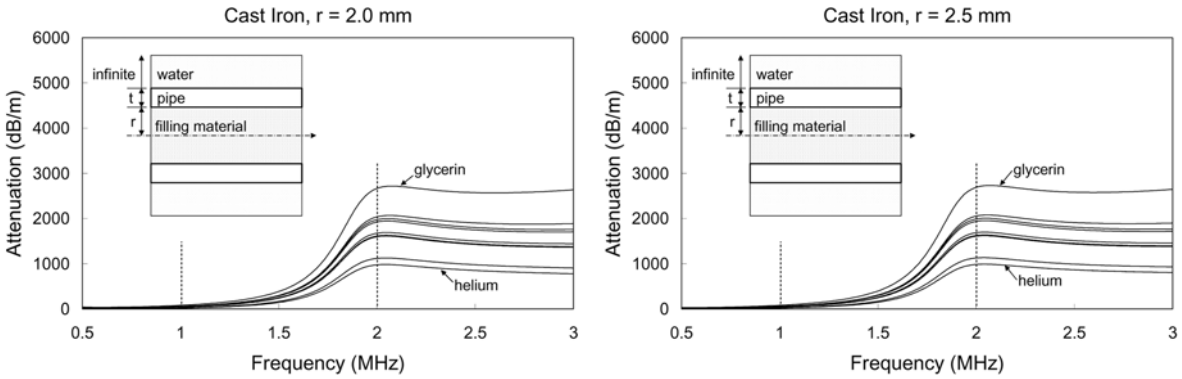

Fig. 2 Frequency vs. attenuation dispersion curves for cast iron pipe with 2.0 mm (left) and 2.5 mm (right) inner radius

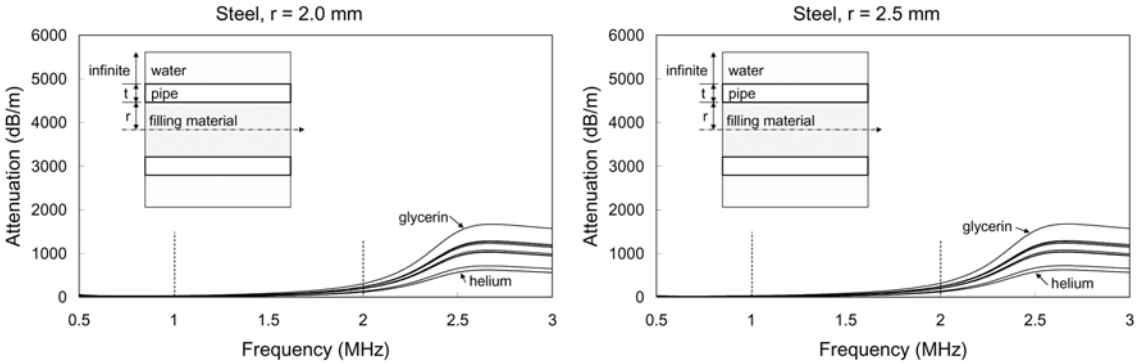

Fig. 3 Frequency vs. attenuation dispersion curves for steel pipe with 2.0 mm (left) and 2.5 mm (right) inner radius

Table 1 Material properties of pipes

Name	Density [kg/m^3]	Longitudinal Velocity [m/s]	Shear Velocity [m/s]
Aluminum	2700	6320	3130
Cast iron	7100	4500	2500
Steel	7932	5960	3260

Table 2 Material properties of filling fluids

Name	Density [kg/m^3]	Longitudinal Velocity [m/s]
Air (at 20°C)	1.205	344
Castor Oil (at 20°C)	971	1474
Diesel Oil	800	1250
Ethyl Alcohol (at 20°C)	790	1238
Glycerin (at 20°C)	1258	1860
Motor Car Oil	870	1740
Water	1000	1500
Kerosene (at 20°C)	822.00	1319.00
Water Steam (at 100°C)	600.00	404.80
Helium (at 25°C)	0.1785	965.00

Fig. 1 shows the attenuation dispersion curves of the fluid filled aluminum pipe in the water; the left figure is for the aluminum pipe having 2.0 mm inner radius and the right figure is for 2.5 mm inner radius. Only fundamental longitudinal wave mode is shown for each filling materials in the figures. These curves show the decay of the guided waves at a certain frequency. The unit of attenuation is dB/m, which means decayed sound intensity per meter. Two frequency values (1 MHz and 2 MHz) are selected for a more detailed analysis and those attenuation values corresponding at radius 2.0 mm and 2.5 mm are shown in Table 3 and Table 4, respectively. Fig. 2 shows the attenuation dispersion curves of the fluid filled cast iron pipe in the water. As the previous, those two frequency values are selected for the detailed analysis and the corresponding attenuation values are shown in Table 5 and Table 6, respectively. Similar work is done for the fluid filled steel pipes in the water as shown in Fig. 3. The

Table 3 Parametric densities and attenuations of L(0,1) mode; 2 mm-radius aluminum pipe is used

Name	Parametric Density (kg/m^3)	Attenuation (dB/m) at 1 MHz	Attenuation (dB/m) at 2 MHz
Air (at 20°C)	99.48	19.44	570.07
Castor Oil (at 20°C)	1392.12	99.75	1075.64
Diesel Oil	1157.12	75.87	920.56
Ethyl Alcohol (at 20°C)	1143.70	74.50	911.10
Glycerin (at 20°C)	1789.40	154.46	1391.90
Motor Car Oil	1367.12	106.56	1085.12
Water	1428.55	104.22	1066.42
Kerosene (at 20°C)	1198.84	81.22	957.92
Water Steam (at 100°C)	715.65	33.30	640.33
Helium (at 25°C)	275.88	19.43	548.60

Table 4 Parametric densities and attenuations of L(0,1) mode; 2.5 mm-radius aluminum pipe is used

Name	Parametric Density (kg/m^3)	Attenuation (dB/m) at 1 MHz	Attenuation (dB/m) at 2 MHz
Air (at 20°C)	99.48	25.46	586.82
Castor Oil (at 20°C)	1392.12	99.02	1105.01
Diesel Oil	1157.12	77.27	945.86
Ethyl Alcohol (at 20°C)	1143.70	75.99	936.17
Glycerin (at 20°C)	1789.40	149.52	1430.67
Motor Car Oil	1367.12	105.51	1115.03
Water	1428.55	103.23	1137.61
Kerosene (at 20°C)	1198.84	82.27	984.15
Water Steam (at 100°C)	715.65	38.23	658.84
Helium (at 25°C)	275.88	25.44	565.02

Table 5 Parametric densities and attenuations of L(0,1) mode; 2 mm-radius cast iron pipe is used

Name	Parametric Density (kg/m^3)	Attenuation (dB/m) at 1 MHz	Attenuation (dB/m) at 2 MHz
Air (at 20°C)	350.12	20.39	976.98
Castor Oil (at 20°C)	2466.08	56.44	1924.83
Diesel Oil	2067.88	44.40	1616.03
Ethyl Alcohol (at 20°C)	2045.70	43.80	1600.78
Glycerin (at 20°C)	3144.60	81.20	2674.75
Motor Car Oil	2634.88	59.92	2040.37
Water	2521.45	58.40	1975.90
Kerosene (at 20°C)	2159.86	46.74	1673.64
Water Steam (at 100°C)	1010.59	24.77	1119.86
Helium (at 25°C)	978.98	18.90	976.85

Table 6 Parametric densities and attenuations of L(0,1) mode; 2.5 mm-radius cast iron pipe is used

Name	Parametric Density (kg/m^3)	Attenuation (dB/m) at 1 MHz	Attenuation (dB/m) at 2 MHz
Air (at 20°C)	350.12	21.68	987.09
Castor Oil (at 20°C)	2466.08	55.71	1937.05
Diesel Oil	2067.88	46.67	1626.10
Ethyl Alcohol (at 20°C)	2045.70	46.09	1610.79
Glycerin (at 20°C)	3144.60	82.80	2694.92
Motor Car Oil	2634.88	59.06	2054.51
Water	2521.45	57.58	1988.44
Kerosene (at 20°C)	2159.86	48.98	1688.13
Water Steam (at 100°C)	1010.59	27.42	1128.28
Helium (at 25°C)	978.98	21.68	985.01

Table 7 Parametric densities and attenuations of L(0,1) mode; 2 mm-radius steel pipe is used

Name	Parametric Density (kg/m^3)	Attenuation (dB/m) at 1 MHz	Attenuation (dB/m) at 2 MHz
Air (at 20°C)	297.15	3.61	117.67
Castor Oil (at 20°C)	2239.08	20.89	230.52
Diesel Oil	1875.38	16.17	193.99
Ethyl Alcohol (at 20°C)	1855.05	15.88	192.16
Glycerin (at 20°C)	2858.16	33.12	312.40
Motor Car Oil	2366.92	22.29	239.69
Water	2290.45	21.88	236.42
Kerosene (at 20°C)	1956.74	17.27	201.12
Water Steam (at 100°C)	948.25	6.62	132.67
Helium (at 25°C)	830.37	3.37	117.94

Table 8 Parametric densities and attenuations of L(0,1) mode; 2.5 mm-radius steel pipe is used

Name	Parametric Density (kg/m^3)	Attenuation (dB/m) at 1 MHz	Attenuation (dB/m) at 2 MHz
Air (at 20°C)	297.15	4.55	118.78
Castor Oil (at 20°C)	2239.08	20.77	238.98
Diesel Oil	1875.38	15.73	201.32
Ethyl Alcohol (at 20°C)	1855.05	15.47	199.43
Glycerin (at 20°C)	2858.16	31.91	323.49
Motor Car Oil	2366.92	21.97	248.47
Water	2290.45	21.58	245.06
Kerosene (at 20°C)	1956.74	16.71	208.67
Water Steam (at 100°C)	948.25	7.19	138.14
Helium (at 25°C)	830.37	4.55	118.78

corresponding attenuation values are shown in Table 7 and Table 8. As a result, it is shown that the attenuations are quite similar over low frequency ranges for each case, but they are different over high frequency ranges. Overall, glycerin filled pipes give the highest attenuation and helium filled pipes give the lowest attenuation. In general, among the three different pipe materials, aluminum pipes give the highest attenuation, and steel pipes give the lowest attenuation. However, at a specific frequency, for example at 2 MHz, cast iron pipes give the higher attenuation than aluminum pipes.

5. Parametric density concept

As shown in the previous section, two frequency values (1 MHz, 2 MHz) are selected to capture the attenuation values and the attenuation values are summarized in the Table 3 to Table 8. However, in the previous section, for each filling fluids, the attenuation dispersion curves should be numerically calculated to capture the attenuation values. This work is quite complex, time consuming; hence, an approximate method is desirable. Therefore, we propose parametric density concept for the attenuation calculations. This concept was originally introduced by Na, *et al*. (2006) but their work is limited to single case so that the extension of this concept is necessary for more strict verification. The definition of parametric density is as follows:

$$\rho_p = \rho_f + \frac{c_f}{c_s^L + c_s^S}\rho_s \tag{5}$$

where, ρ_p is the parametric density, ρ_p is the density of a filling fluid, ρ_f is the longitudinal wave velocity of the fluid, c_s^L is the longitudinal wave velocity of solid, c_s^S is the shear wave velocity of solid, and ρ_s is the density of solid. In the case of aluminum pipe, by substituting the material properties given in Table 1, c_s^L = 6320 m/sec, c_s^S = 3130 m/sec, and ρ_s = 2700 kg/m^3 into Eq. (5), the equation becomes

$$\rho_p = \rho_f + 0.2857 c_f \tag{6a}$$

Similar calculations can be done for the cast iron and steel pipe, respectively; those equations are as follows:

$$\rho_p = \rho_f + 1.0143 c_f \tag{6b}$$

$$\rho_p = \rho_f + 0.8603 c_f \tag{6c}$$

Once the equation above is set, it is ready to obtain parametric versus attenuation curves. First, by using Eq. (6a), those parametric densities for 2 mm thick aluminum pipes are calculated and shown in Table 3. Second, only three attenuation values, obtained from the previous section, for glycerin, diesel oil, and air filled aluminum pipes are selected and plotted on Fig. 4 (denoted by solid diamonds). This selection is not done in a random way. The glycerin and air are chosen because they give the highest and lowest parametric densities, respectively, and diesel oil is selected because its parametric density is a kind of medium value. Third, the trend line of these three points is constructed by a 2nd degree polynomial. This fitting is done since the 2nd degree polynomial is one of the simplest ways to the curve fitting. Finally, to verify the trend, the attenuation values, obtained from the previous section, for other seven filling fluids

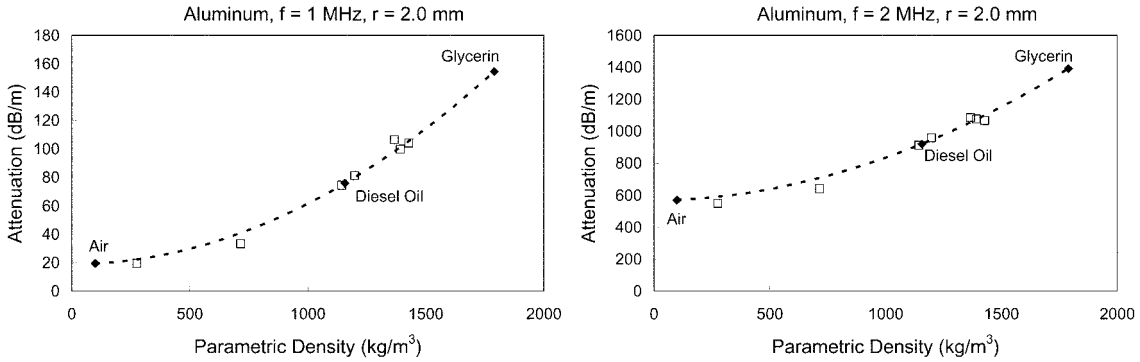

Fig. 4 Parametric density vs. attenuation curve for aluminum pipe with 2 mm inner radius at 1 MHz (left) and 2 MHz (right), respectively

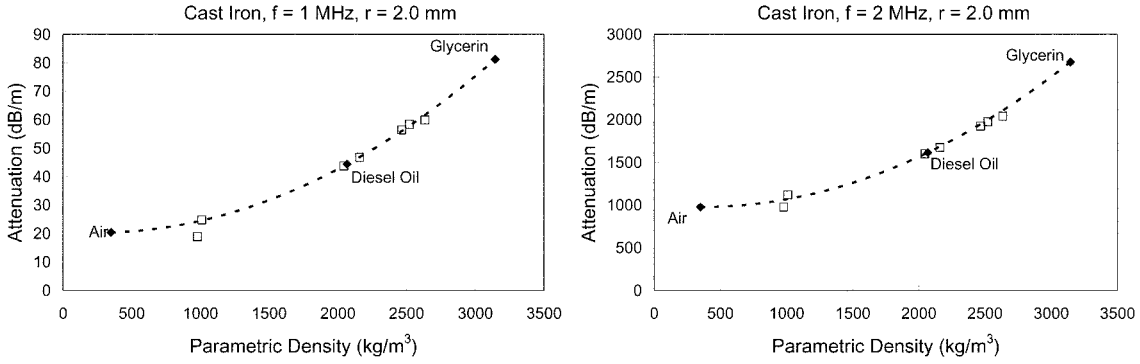

Fig. 5 Parametric density vs. attenuation curve for cast iron pipe with 2 mm inner radius at 1 MHz (left) and 2 MHz (right), respectively

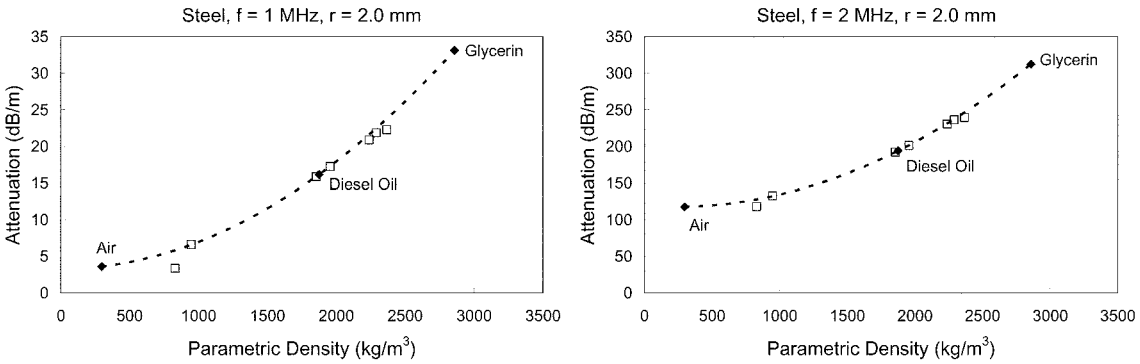

Fig. 6 Parametric density vs. attenuation curve for steel pipe with 2 mm inner radius at 1 MHz (left) and 2 MHz (right), respectively

are plotted on Fig. 4 (denoted by hollow squares). From the figure, it is shown that the 2nd degree polynomial approximates those attenuation values quite well. In other words, if we know a parametric density of a certain pipe then we can obtain the attenuation value from the parametric density versus attenuations curves without numerically solving the dispersion equation.

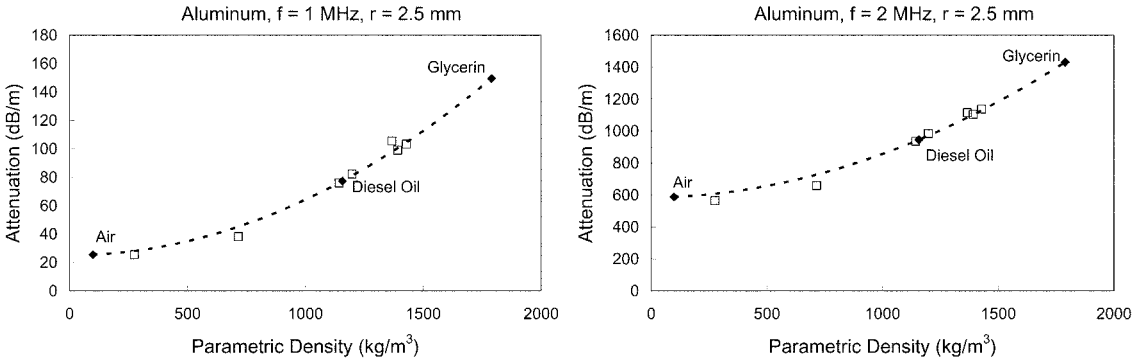

Fig. 7 Parametric density vs. attenuation curve for aluminum pipe with 2.5 mm inner radius at 1 MHz (left) and 2 MHz (right), respectively

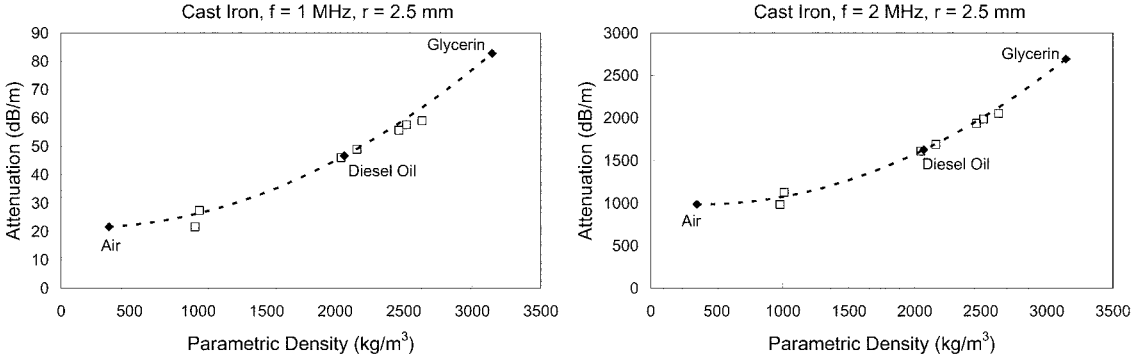

Fig. 8 Parametric density vs. attenuation curve for cast iron pipe with 2.5 mm inner radius at 1 MHz (left) and 2 MHz (right), respectively

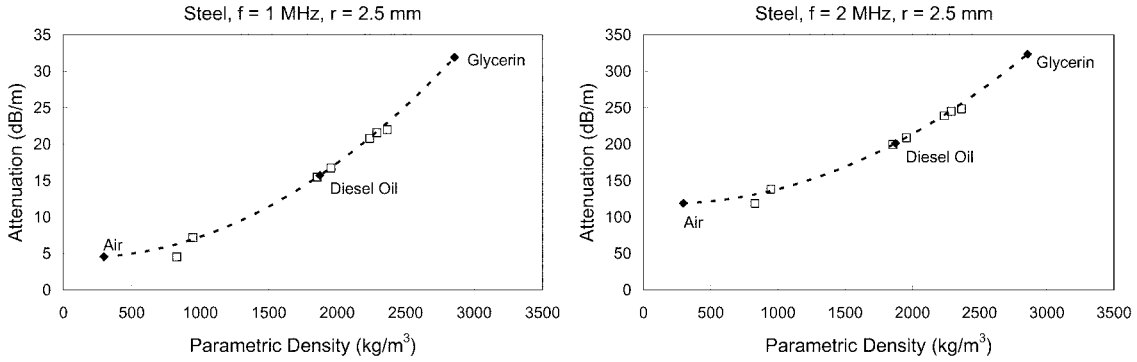

Fig. 9 Parametric density vs. attenuation curve for steel pipe with 2.5 mm inner radius at 1 MHz (left) and 2 MHz (right), respectively

Similar works, by using Eqs. (6b) and (6c), are done as shown in Figs. 5 to 6. In spite of the different pipe materials, the parametric density versus attenuation curves show how the trend lines reasonably match with the attenuation values. In addition, in Figs. 7, 8, and 9, it is shown that the parametric density concept is useful regardless the size of inner radius of each pipelines. Those results are shown

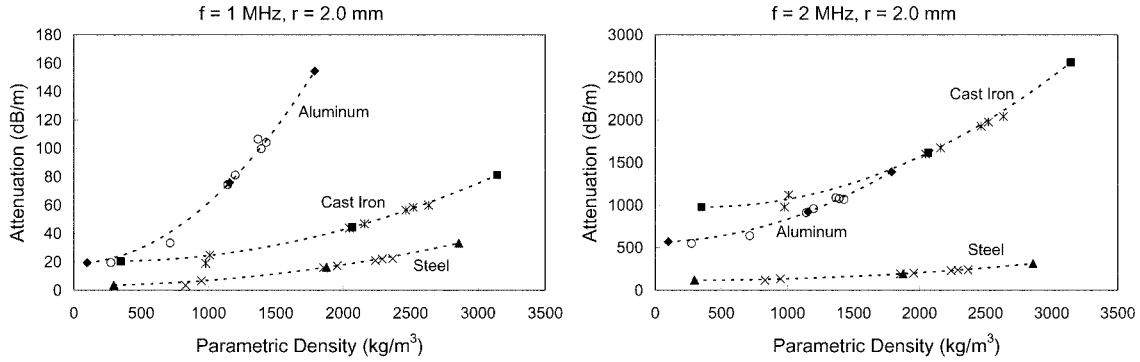

Fig. 10 Parametric density vs. attenuation curve for three pipes with 2 mm inner radius at 1 MHz (left) and 2 MHz (right), respectively

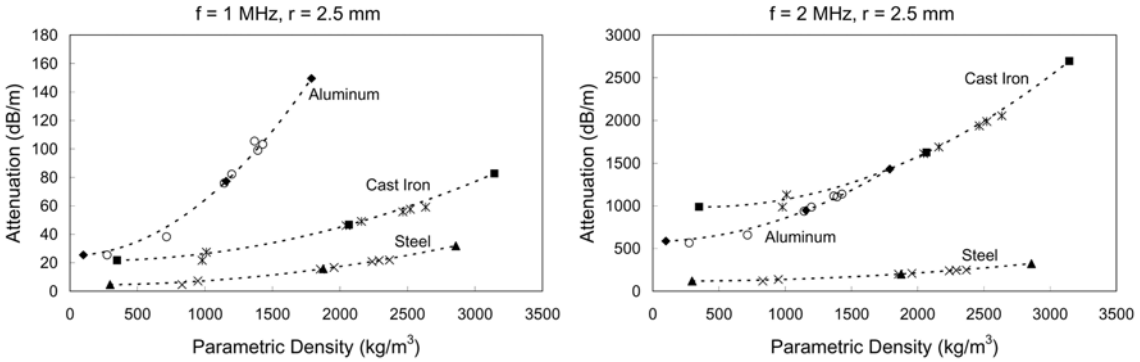

Fig. 11 Parametric density vs. attenuation curve for three pipes with 2.5 mm inner radius at 1 MHz (left) and 2 MHz (right), respectively

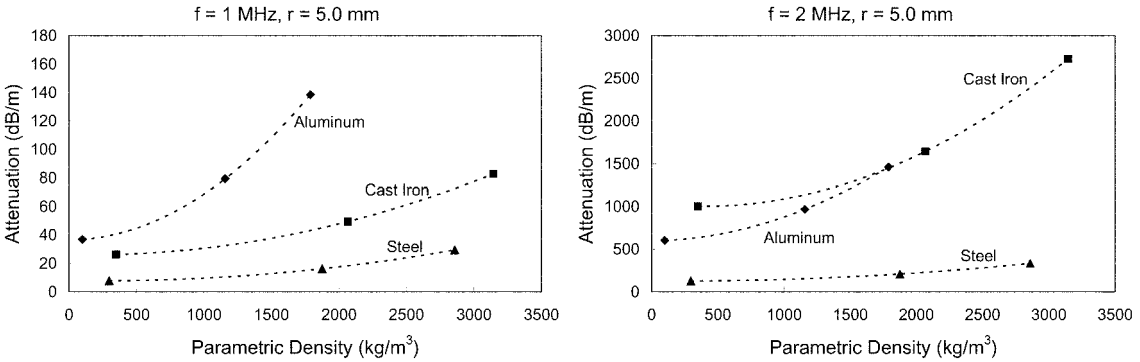

Fig. 12 Parametric density vs. attenuation curve for three pipes with 5.0 mm inner radius at 1 MHz (left) and 2 MHz (right), respectively

again in Figs. 10 and 11 for the comparison purpose. It is shown that the aluminum pipelines give the highest attenuations at 1 MHz, but the cast iron pipelines give the highest attenuation at 2 MHz for both 2 mm and 2.5 mm inner radii. To see the effect of inner radius on the parametric density versus attenuation, two more inner radii such as 5 mm and 10 mm, are considered, and the parametric density

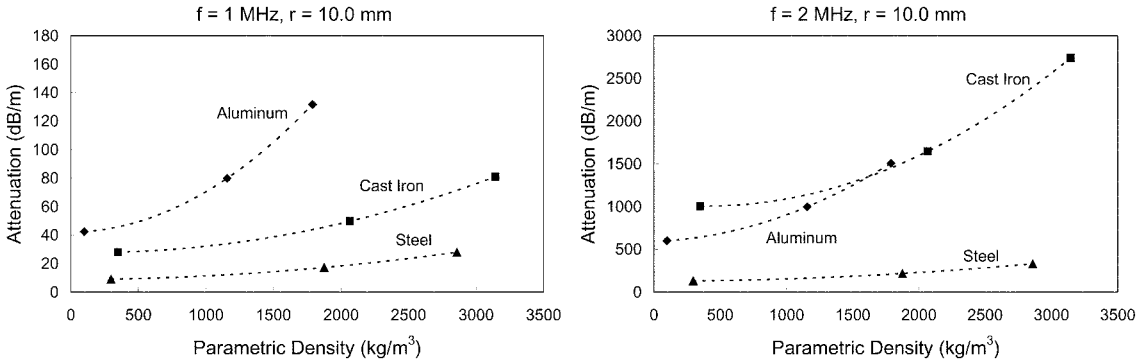

Fig. 13 Parametric density vs. attenuation curve for three pipes with 10.0mm inner radius at 1 MHz (left) and 2 MHz (right), respectively

versus attenuation curves are shown in Figs. 12, and 13. In those cases, only three points corresponding to glycerin, diesel oil, and air-filled pipes are plotted. Then, once we know a parametric density from Eq. (5), the associated attenuation value is obtainable from the figure. It is emphasized here that the size of inner radius does not severely affect the attenuation values for fluid-filled pipes surrounded by water as shown in Fig. 10 to Fig. 13. In other words, the ratio of inner radius to pipe wall thickness is not a significant factor on the guided wave attenuations. That is because the most attenuation is caused by the filling fluids inside and the water surrounding the pipelines.

In summary, Eq. (5) is reasonable to predict the attenuation values, which are function of the parametric density. In other words, once the parametric density of a pipe with a certain filling fluid is obtained, we can predict the attenuation of L(0,1) mode for the fluid-filled pipe at 1 MHz or 2 MHz, respectively. This approach may not be limited to the two specific frequencies; other frequencies can be dealt with the same approach. However, it should be noted here that the parametric density concept is not verified yet for other dispersion curves such as phase velocity and group velocity. Besides, a theoretical verification of the parametric concept has not been finished yet; hence, it remains in the future work.

6. Conclusions

Parametric density concept is proposed for a long-range pipeline health monitoring. This concept is designed to obtain the attenuation of ultrasonic guided waves propagating in underwater pipelines without complicated calculation of attenuation dispersion curves. For the study, three different pipe materials such as aluminum, cast iron, and steel are considered, ten different transporting fluids such as glycerin, diesel oil, etc. are assumed, and four different geometric pipe dimensions, 2.0, 2.5, 5.0, 10.0 mm, are adopted. It is shown that the attenuation values based on the parametric density concept reasonably match with the attenuation values obtained from dispersion curves; hence, its efficiency is verified. With this concept, field engineers or inspectors associated with long-range pipeline health monitoring would take the advantage of easier capturing wave attenuation value, which is a critical variable to decide sensor location or sensors interval.

Acknowledgement

This work was supported by Pukyong National University Research Fund in 2005 and 2006.

References

Achenbach, J. D. (1984), *Wave Propagation in Elastic Solids*, North-Holland.
Alleyne, D. N. and Cawley, P. (1996), "The excitation of lamb waves in pipes using dry-coupled piezoelectric transducers", *J. Nondestruct. Eval.*, **15**, 11-20.
Aristégui, C., Lowe, M. J. S., and Cawley, P. (2001), "Guided waves in fluid-filled pipes surrounded by different fluids", *Ultrasonics*, **39**, 367-375.
Balageas, D. (2006), "Introduction to structural health monitoring", Eds. Balageas, D., Fritzen, C. P., and Guemes, A., *Struct. Health Monit.,* 13-43, ISTE.
Gazis, D. C. (1959a), "Three dimensional investigation of the propagation of waves in hollow circular cylinders ii. numerical results", *J. Acoust. Soc. Am.*, **31**, 573-578.
Gazis, D. C. (1959b), "Three dimensional investigation of the oropagation of waves in hollow circular cylinders", *J. Acoust. Soc. Am.*, **31**, 568-572.
Guo, D., and Kundu, T. (2001), "A new transducer holder mechanism for pipe inspection", *J. Acoust. Soc. Am.*, **110**, 303-309.
Knopoff, L. (1964), "A matrix method for elastic wave problems", *Bulletin Seismol. Soc. Am.*, **54**, 431-438.
Kolsky, H. (1963), *Stress Waves in Solids*, Dover.
Kumar, R. (1971), "Flexural vibrations of fluid-filled circular cylindrical shells", *Acustica*, **24**, 137-146.
Kwun, H. and Crouch, A. (2006), "Guided wave fills inspection gap", *Pipeline and Gas Technology*, **August**, 28-31.
Kwun, H., Bartels, K. A., and Dynes, C. (1999), "Dispersion of longitudinal waves propagating in liquid-filled cylindrical shells", *J. Acoust. Soc. Am.*, **105**, 2601-2611.
Kwun, H., Kim, S. Y., Choi, M. S., and Walker, S. M. (2004), "Torsional guided-wave attenuation in coal-tar-enamel-coated, buried piping", *NDT&E Int.*, **37**, 663-665.
Lowe, M. (1995), "Matrix techniques for modeling ultrasonic waves in multilayered media", *IEEE Transactions on Ultrasonics, Ferroelectrics, Frequency Control*, **42**, 525-542.
Mal, A. (1988), "Wave propagation in layered composite laminates under periodic surface loads", *Wave Motion*, **10**, 257-266.
Meeker, T. R. and Meitzler, A. H. (1972), "Guided wave propagation in elongated cylinder and plates", Eds. Mason, W. P. and Thurston, R. N., *Physical Acoustic Principles and Methods*, **1A**, 111-167, New York, Academic Press.
Na, W. B. and Kundu, T. (2002), "Wave attenuation in pipes and its application in determining axial spacing of monitoring sensors", *Mater. Eval.*, **60**, 635-644.
Na, W. B., Ryu, Y. S., and Kim, J. T. (2005), "Attenuation of fundamental longitudinal cylindrical guided wave propagating in liquid-filled steel pipes", *J. Ocean Eng. Tech.*, **19**, 26-33.
Na, W. B., Kim, J. T., Yoon, H. S., and Hong, D. S. (2006), "Pipeline sensor location determination based on guided wave propagation", *Proceedings of the Seventh ISOPE Pacific/Asia Offshore Mechanics Symposium*, Dalian, China, Sep. 335-340.
Nagy, P. B. (1995), "Longitudinal guided wave propagation in a transversely isotropic rod immersed in fluid", *J. Acoust. Soc. Am.*, **98**, 454-457.
Onoe, M., McNiven, H. D., and Mindlin, R. D. (1962), "Dispersion of axially symmetric waves in elastic solids", *J. Appl. Mech.*, **29**, 729-734.
Pan, E., Rogers, J., Datta, S. K., and Shah, A. H. (1999), "Mode selection of guided waves for ultrasonic inspection of gas pipelines with thick coating", *Mech. Mater.*, **31**, 165-174.
Pavlakovic, B. and Lowe, M. (2001), *DISPERSE: User's Manual*, Imperial College, University of London, Non-Destructive Testing Laboratory.

Pavlakovic, B. N., Lowe, M. J. S., Alleyne, D. N., and Cawley, P. (1997), "Disperse: a general purpose program for creating dispersion curves", Eds. D.O. Thompson and D.E. Chimenti, *Review of Progress in Quantitative Nondestructive Evaluation*, **18**, 239-246, Plenum Press, New York.

Randall, M. J. (1967), "Fast programs for half-space problems", *Bullet. Seismol. Soc. Am.*, **57**, 1299-1315.

Rose, J. L. (1999), *Ultrasonic Waves in Solid Media*, Cambridge University Press.

Rose, J. L., Ditri, J. J., Pilarski, A., Rajana, K., and Carr, F. (1994), "A guided waves inspection technique for nuclear steam generator tubing", *NDT&E Int.*, **27**, 307-310.

Schmidt, H. and Jensen, F. B. (1985), "A full wave solution for propagation in multilayered viscoelastic media with application to gaussian beam reflection at liquid-solid interfaces", *J. Acoust. Soc. Am.*, **77**, 813-825.

Scott, S. L. and Barrufet, M. A. (2003), *Worldwide Assessment of Industry Leak Detection Capabilities for Single and Multiphase Pipelines*, Offshore Technology Research Center.

Wilcox, P., Lowe, M., and Cawley, P. (2001), "The effect of dispersion on long-range inspection using ultrasonic guided waves", *NDT&E Int.*, **34**, 1-9.